

Kuiper Belt: Utilizing the “Out-of-natural Angle” Region in the Eye-gaze Interaction for Virtual Reality

Myunguen Choi
Hokkaido University
Sapporo, Hokkaido, Japan
myunguen.choi.p4@elms.hokudai.ac.jp

Daisuke Sakamoto
Hokkaido University
Sapporo, Hokkaido, Japan
sakamoto@ist.hokudai.ac.jp

Tetsuo Ono
Hokkaido University
Sapporo, Hokkaido, Japan
ono@ist.hokudai.ac.jp

ABSTRACT

The maximum physical range of horizontal human eye movement is approximately 45° . However, in a natural gaze shift, the difference in the direction of the gaze relative to the frontal direction of the head rarely exceeds 25° . We name this region of 25° – 45° the “Kuiper Belt” in the eye-gaze interaction. We try to utilize this region to solve the Midas touch problem to enable a search task while reducing false input in the Virtual Reality environment. In this work, we conduct two studies to figure out the design principle of how we place menu items in the Kuiper Belt as an “out-of-natural angle” region of the eye-gaze movement, and determine the effectiveness and workload of the Kuiper Belt-based method. The results indicate that the Kuiper Belt-based method facilitated the visual search task while reducing false input. Finally, we present example applications utilizing the findings of these studies.

CCS CONCEPTS

• Human-centered computing → Virtual reality; Pointing.

KEYWORDS

Eye-gaze Interface; Virtual Reality; Eye Tracking; Menu Item Selection

ACM Reference Format:

Myunguen Choi, Daisuke Sakamoto, and Tetsuo Ono. 2022. Kuiper Belt: Utilizing the “Out-of-natural Angle” Region in the Eye-gaze Interaction for Virtual Reality. In *CHI Conference on Human Factors in Computing Systems (CHI '22)*, April 29–May 5, 2022, New Orleans, LA, USA. ACM, New York, NY, USA, 17 pages. <https://doi.org/10.1145/3491102.3517725>

1 INTRODUCTION

In the field of human-computer interaction, the exploration of novel input methods using head-mounted displays (HMDs) in the domains of virtual reality (VR) and mixed reality (MR) is an active area of research. The current main input methods which enable the generation of characters unavailable on input devices, are hand-based, such as controllers [2], gestures [5, 36], and touch pads [14]. However, long-term hand interaction causes hand fatigue, referred to as the *gorilla-arm effect* [3, 18]. Thus, various hands-free input

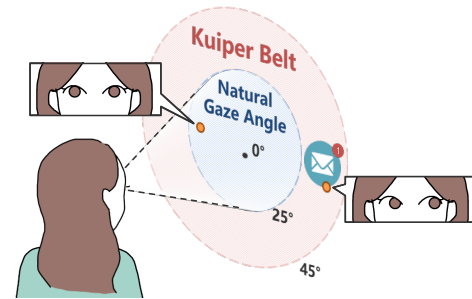


Figure 1: Kuiper Belt in VR interaction: We utilize the unnatural gaze shift to reduce the Midas touch problem in an eye-gaze interface.

methods have been studied, such as head [8], foot [38, 62] and eye-gaze [6, 56] dependent techniques.

The eye-gaze interface is one of the promising input methods because it is fast and the eye-tracker can be naturally mounted onto the HMD. However, monomodal gaze input has a problem called the “Midas touch problem” [23] whereby a target is selected against the user’s intention due to the inability to distinguish between gaze fixation for the purpose of selection or examination. Researchers have presented techniques to solve this problem, such as, dwell-time adjustment [32, 37, 42, 59], gaze-stroke gestures [7, 22], and smooth pursuits [46, 58]. These studies reduced the error rate (Midas touch) by comparison in the standard dwell time-based eye-gaze interfaces; however, there are trade-offs such as lower error rates, longer dwell times, and/or task completion time. We also address this problem by utilizing a new region referred to as “Kuiper Belt” in eye-gaze interaction research to achieve a lower error rate and lower dwell time.

Our goal is to figure out the design principle of the Kuiper Belt menu item placement method to solve the Midas touch problem during visual search tasks in the VR and MR environments, trying to determine where to place the menu items within the area of the large angle between the eye and head (Figure 1). Initially, we explore the design principle of “out-of-natural angle” region utilization for menu item selection. In Study #1, we investigate how to place menu items in the region of the Kuiper belt. The result showed that the Kuiper belt was not a true circle shape; the menu items need to be placed slightly closer to the center for the upward direction compared to the downward direction in the circle. In Study #2, we validate our concept of how to use the Kuiper Belt method, considering its workload, to solve the Midas touch problem. We measure the effectiveness and workload of the Kuiper Belt menu

Permission to make digital or hard copies of all or part of this work for personal or classroom use is granted without fee provided that copies are not made or distributed for profit or commercial advantage and that copies bear this notice and the full citation on the first page. Copyrights for components of this work owned by others than the author(s) must be honored. Abstracting with credit is permitted. To copy otherwise, to republish, to post on servers or to redistribute to lists, requires prior specific permission and/or a fee. Request permissions from permissions@acm.org.

CHI '22, April 29–May 5, 2022, New Orleans, LA, USA

© 2022 Copyright held by the owner/author(s). Publication rights licensed to ACM.

ACM ISBN 978-1-4503-9157-3/22/04...\$15.00

<https://doi.org/10.1145/3491102.3517725>

placement method by comparing it to other methods. The results showed that the Kuiper Belt can reduce the Midas touch during a visual search task.

The key idea of the Kuiper Belt menu item placement method is that gaze shift is performed by moving the eyes, head, and torso. In particular, gaze shifts of less than 20° occur almost exclusively through the eyes [12, 13]. The eyes rarely rotate beyond 25° relative to the head [11, 50, 54] although they are able to move farther; the maximum physical range is approximately 45° [53, 54]. Thus, humans rarely hold their eyes at angles exceeding 25° unless the movement is intentional. In other words, gaze interaction at this angle is unlikely to cause the Midas touch problem.

Our contributions are as follows:

- Explored design principle of how to place menu items in the “Out-of-natural Angle” region named Kuiper Belt, where large eye and head movement angles are required.
- Investigated the effectiveness of the Kuiper Belt menu item placement method in terms of usability and workload, and confirmed that the Kuiper Belt method can reduce false input (Midas touch) in an eye-gaze interface.
- Presented four applications of the Kuiper Belt to illustrate its potential.

2 RELATED WORK

2.1 Methods to Solve the Midas Touch Problem

Research on eye-gaze interaction and gaze-based interfaces has a long history. Researchers have been trying to solve the Midas touch problem to create an accurate target- and menu-selection method. Herein, we briefly review previously presented studies in the field of gaze-based interfaces. Table 1 provides an overview of existing solutions and our work to address the Midas touch problem.

2.1.1 Selection by combining eye-gaze input and other modalities. A popular method of solving the Midas touch problem is to combine the gaze with other modalities. The user can avoid unintentional selection by using gaze to indicate the target while executing the decision trigger in another modality. Other modalities include clicking a mouse [65], making a foot gesture [16], clicking via a tooth switch [67], and using a facial-EMG switch [55]. Explicit triggers in multimodal interaction are easy to understand and use. Similarly, various methods of combining gaze and other input interfaces in VR and MR have been proposed [27, 41], especially based on the combination of head movements and gaze [49]. The combination of eye and head movement as an input method is suitable for VR and MR because both eye and head movements can easily be tracked simultaneously with an HMD and the user can point and select targets without using either hand.

2.1.2 Selection method employing dwell time. In monomodal gaze interfaces, the most common method selects a target when the gaze dwells on that target for a certain period of time. When the dwell time was set to 150 ms, the gaze input achieved faster target selection than the mouse [47]. On the other hand, shortening the dwell time led to frequent false inputs, so the dwell time was set to between 450 ms and 1000 ms for each study of eye-typing [34]. Since the longer the dwell time, the longer the movement time, in order to solve the Midas touch problem and reduce the dwell time,

the user manually adjusted the dwell time [32, 59], for each key according to the input options [37, 42].

2.1.3 Separation of targets and labels. These studies adopted experimental tasks in which the targets to be selected were either clearly highlighted or were visually- and positionally-fixed like an eye-typing keyboard. However, for complex but practical tasks, the user had to visually search a desired- and positionally-unfixed target object among various objects; we refer to this target selection task, as a “visual search task.” Zhang *et al.* confirmed that complex visual search increases the required dwell time [66]. The experimental task was to select a target with the specified label from seven candidate targets, each with a label written inside the target. The error rate of this experiment was 16.9% when the difficulty of visual search was complex and the dwell time was 1100 ms. Pfeuffer *et al.* also confirmed that a dwell time of 1000 ms was not sufficient (the error rate was 9.72%) for a visual search task, and a dwell time of 2000 ms was preferable [40]. Hence, setting a long dwell time is not enough to solve the Midas touch problem when the difficulty of the task is high.

One of the reasons for the high error rate in the experimental task of Zhang *et al.* [66] was that the labels were written inside the target. Penkar *et al.* [39] found that separating the target from the label reduced the Midas touch rate of the task, and that the Midas touch rate was 0 when the dwell time was short (200 ms). As one of the eye-gaze input methods that separates target and label, Lutteroth *et al.* [31] proposed Actigaze, a method to select links in hypertext by gaze alone. This method separates the text containing the hyperlink (label) from the hyperlink selection button (target), so that Midas touch does not occur during visual search for a given hyperlink. With Actigaze, the median click times were fairly close to the mouse click times and a low error rate of less than 4% was achieved, even though the dwell time during target selection was 200 ms.

Therefore, separating a target from a label is effective in solving the Midas touch problem during visual search tasks. However, previous works have been conducted with a graphical user interface in a 2D display environment, and not in 3D virtual reality environments. In 2D GUI interaction, it is relatively easy to separate a target from a label because we can design an application screen to separate areas of targets and labels. However, in 3D VR interaction, it is not simple to separate them because all areas are within the visual search space. We aim to separate the targets and labels in the VR environment by utilizing the “out-of-natural angle” region, which is the key to the Kuiper Belt interface design principle.

2.2 Distribution and Characteristics of Gaze

The angular difference between the eye and head is generally within 25° , which is a comfortable zone for humans; the human eye does not frequently move outside of this region in natural eye movement. Hu *et al.* found that 98.7% of the gaze data lie in the central 17.5° region in dynamic virtual scenes [20], and Foulshama *et al.* found that most of the gaze data of people walking were within 25° of each other [11].

The maximum physical range of horizontal eye movement is approximately 45° (More precisely 46.4° CI [44.0; 48.8]) [53, 54]. Stahl *et al.* hypothesized that extreme eye angles are rarely used and

Table 1: An overview existing solutions to solve the Midas touch problem.

	Use Case	Physical Fatigue	Selection	Visual Search	Speed	Environment
Dwell Time [23]	Object Selection	Low	High	Low	Modelate	VR, PC
Smooth Pursuit [46, 58]	Object Selection	Modelate	Modelate	Modelate	Low	VR, PC
Gaze Pointing + Other Modality [26, 60]	Object Selection	High	High	High	High	VR, PC
Eye & Head [49]	Object Selection	High	High	High	Modelate	VR
Radi-Eye [52]	Object Selection + Command Activation	High	High	High	Low	VR
SPOCK [46]	Object Selection	Modelate	High	High	Low	PC
ActiGaze [31]	Object Selection	Modelate	High	High	High	PC
Outline Pursuit [48]	Object Selection	High	Low	Low	Low	VR
EyeSeeThrough [35]	Object Selection + Command Activation	High	High	High	Low	VR
Gaze+Hold [43]	Object Selection + Command Activation	High	Modelate	Modelate	Low	PC
Kuiper Belt	Object Selection + Command Activation	High	Modelate	Modelate	High	VR

ocular kinematics worsen as ocular eccentricity increases [53]. For instance, saccades to more eccentric positions are less accurate [63] and about 50% of normal subjects develop end-point nystagmus (EPN with amplitudes ranging between 0.2° and 2.5°) when the angular difference between the eye and head is beyond 30° of eccentricity [1]. In addition, as this angle increases, accuracy of the eye tracker decreases and the required target size to be selected increases¹. Therefore, the characteristics of gaze at an ocular eccentricity of 30° or more are different from those of natural ocular eccentricity. In this work, we try to understand the characteristics of this “out-of-natural angle” region in eye-gaze interaction and to find a design principle for the eye-gaze interface in the VR environment.

2.3 Region for Gaze Interaction in VR and MR

In VR and MR, the selectable targets are usually located within windows fixed to the (1) HMD, (2) surrounding information, and (3) locations and objects in the 3D world [9]. Basically, many of the eye-gaze pointing methods are for targets that are fixed to the surrounding information (2) (3) because many eye-gaze pointing methods are based on the premise of interaction with a fixed display. However, there are also a few eye-gaze pointing methods that select an HMD-mounted target [21, 30, 35, 57], which is fixed to the user’s head and is always in the same position within the user’s field of view. The advantage of gaze interaction with an HMD-mounted target is that the user can immediately gaze at the target, but Midas touch does occur [30] because of the small angular difference between the target and the user’s head.

In all of the aforementioned methods, the target is positioned at an angle of less than 20° difference between the eyes and the head (Ishiguro *et al.* [21] ($< 18.5^\circ$); Tonnis *et al.* [57] (8°); Lu *et al.* [30] ($< 20^\circ$); Mardanbegi *et al.* [35] (20°)). Similarly, due to the size of the target itself, the angle at which the user’s gaze has to move is smaller. Thus, the position of the target in these methods lies

within the natural human gaze area, where the angular difference between the eye and head is less than 25° . In contrast, the maximum physical range of the human eye movement is about 45° . Therefore, we suggest that by using the region in which the angular difference between the eye and the head ranges from 25° to 45° , it is possible to solve the Midas touch problem while creating a comfortable interface.

2.4 Utilizing “Out-of-natural Angle” region for the Eye-gaze Interaction: Our contribution

The key concept of our work is to utilize the Kuiper Belt, a region that requires large eye movements, to reduce false inputs, i.e., the Midas touch problem, which has not been actively researched so far. This region, which the eyes do not frequently reach, is highlighted in our work as a promising field in the eye-gaze interaction research.

Saidi *et al.* [44] found that the head and eye angle was approximately 30° from the FOV of HoloLens 1 (Vertical 17.5° diameter) the widest distance where the smartphone in the downward direction could be comfortably looked at, without moving the head. This research is not a study of eye-gaze interface, but suggests that an eye-gaze interface for regions requiring large eye movements can be useful. The zone, which we refer to as Kuiper Belt (Figure 2), includes a region where users are able to select objects effectively. We explore this design space with a user study #1. We define the Kuiper Belt as an eye angle between 25° and 45° with respect to the head. This is because the eye angle to the head is rarely more than 25° [11, 50, 54], and the physical range of eye movement is approximately 45° [53, 54].

Next, we conduct another user study #2 to investigate how the Kuiper belt method with the visual search task reduces not only false inputs (Midas touch problem) but also the extent of user strain (mental and physical workload). The Kuiper Belt is a method that focuses on the position of the eyes and head in the gaze. Similar methods have been presented that focus on the relationship between the eye and head movement, such as Eye&Head [49] and

¹Tobii’s internal test <https://vr.tobii.com/sdk/eye-behavior/hardware-accuracy/>



Figure 2: Potential area of the Kuiper Belt

Radi-Eye [52], which combine head and gaze input. These methods have enabled visual search using head movements and a gaze shift within 20° . In contrast, our work aims to utilize the “out-of-natural angle” region where the angular difference between the eyes and head is from 25° to 45° to enable a visual search. We compare three methods: a Kuiper Belt-based menu-selection method, a menu-selection method within the comfort zone ($< 25^\circ$), and a baseline method (two-step menu-selection method). Finally, we discuss the characteristics and limitations of the Kuiper Belt-based menu-selection method in VR.

3 STUDY #1: EXPLORING DESIGN PRINCIPLE OF MENU ITEM PLACEMENT IN KUIPER BELT

We conduct a user study to explore the appropriate menu item placement distance and angle when performing gaze interactions that utilize the “out-of-natural angle” region, herein named the Kuiper Belt. This study was conducted in early 2020 (before the COVID-19 pandemic).

3.1 Apparatus

The experiment was conducted using an Intel Core i9-9750H 2.60 GHz and NVIDIA GeForce RTX 2070 running Windows 10. The task used in the study was developed in Unity Version 2018.3.0f2. We used the HTC Vive Pro Eye, which is equipped with an eye tracker running at 120 Hz. The HTC Vive Pro Eye has a field of view (FOV) of 100° and 110° in the horizontal and vertical plane, respectively, and a frame rate of 90Hz. Therefore, we obtained the gaze data at 90 Hz.

3.2 Participants

A total of 10 participants (one female, mean age 22.7 years, $SD = 1.4$ years) were enrolled. All had normal or corrected-to-normal vision, and all had prior experience with an eye-tracking interface. This experiment utilizes the out-of-natural region of eye gaze movement, where the eye-gaze extends beyond the area of the eyeglasses. The eye tracker is not able to track participants' eye gaze outside this region. Therefore, a person with eyeglasses could not participate in this study because no one in this experiment wore any type of eyeglasses. However, five of the participants wore contact lenses. Each participant received a US\$ 10 gift voucher, and each study took approximately 40 min.

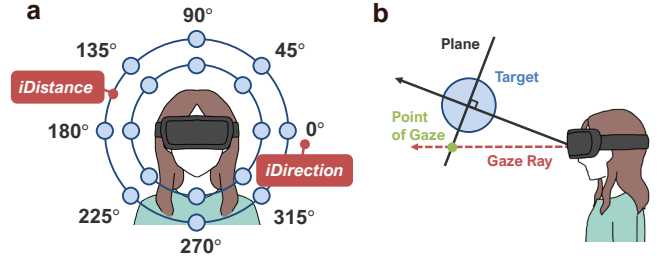


Figure 3: a) Independent variables. b) Definition of point of gaze.

3.3 Design

We used a within-participant design. The two independent variables (Figure 3 (a)) were as follows:

- Menu Item Distance (*iDistance*; $12^\circ, 22^\circ, 32^\circ, 37^\circ, 42^\circ$)
- Menu Item Direction (*iDirection*; $0^\circ, 45^\circ, 90^\circ, 135^\circ, 180^\circ, 225^\circ, 270^\circ, 315^\circ$)

For *iDistance* values, we adopted 12° and 22° , which are within the natural eye angle relative to the head, and $32^\circ, 37^\circ$, and 42° , which are sufficiently outside the natural eye angle considered as part of the Kuiper belt. This is because we would like to compare the Kuiper Belt with the normal viewing area. Since the goal of this study is to explore the design principle in the region of the Kuiper Belt, we adopted parameters with narrower intervals for angles corresponding to the Kuiper Belt ($32^\circ, 37^\circ, 42^\circ$) and wider intervals for angles corresponding to the normal viewing area ($12^\circ, 22^\circ$).

iDistance was the principal independent variable, and each participant experienced each *iDistance* three times (for a total of 15 sessions using five *iDistances*). The order of the *iDistance* was counterbalanced using a Latin square. The order of the eight *iDirection* values in one session was random. The participants were able to take a break between sessions. Finally, we collected $5 \text{ } iDistance \times 3 \text{ times} \times 8 \text{ } iDirection = 120$ valid menu-item-selection datasets for each participant (1,200 datasets in total).

We collected gaze data to investigate the menu item size required to enable robust interaction in the Kuiper Belt. As the gaze angle increases, its accuracy decreases and the required menu item size increases. The menu item size required to enable robust interaction is defined as the spherical radius where, for 75% of fixations, at least 90% of gaze points fall inside the menu item.

The dependent variables were the error rate, physical comfort, mental comfort, and NASA-TLX questionnaire items. If an incorrect menu item was selected or a trial took more than 5.0 s, the trial was considered erroneous. The physical and mental comfort questionnaires quantified how the user's comfort level (physical and mental) changed for each combination of *iDistance* and *iDirection*, referring to [62]. To collect data, a 5-point scale (from 1 "strongly agree" to 5 "strongly disagree") was used with respect to mental and physical comfort ("I felt mental or physical fatigue after the pointing task was completed."). Finally, we used NASA Task Load Index (NASA-TLX) [15] questionnaires assessing the workload for each *iDistance*.



Figure 4: Experimental setup, and what participants see in the VR environment with HMD.

3.4 Procedure and Task

First, we welcomed the participant and then briefly introduced the study to them. All participants provided written and informed consent. We provided detailed task instructions using graphical images. The participants performed 5-point eye-tracking calibration of the initially installed program on the HTC Vive Pro Eye. All participants engaged in a practice session prior to the main sessions; different parameters ($iDistance = 10^\circ$) were used for the practice session.

The task is a pointing task, in which the participant repeatedly selects a menu item fixed to the participant’s HMD, wherein the menu items are always in the same position in the user’s FOV. The task was initiated once the participant dwelled on a menu item generated right in front of the face within $\pm 1.5^\circ$ for 0.4 s (Dwell Time: 400 ms). After that, the central menu item disappeared and a new menu item was generated. An arrow pointing in the direction of the new menu item was also generated at the position of the central menu item. The menu item was a 1.0° radius sphere placed in a hemisphere 2.0 m from the HMD. When the user gazed at the menu item, as feedback, the menu item changed from white to red and a circular slider [29] was drawn around the menu item to indicate dwell time (Figure 4). Participants were instructed to dwell on the new menu item as quickly and accurately as possible. The menu item disappeared when the participant dwelled on the menu item within $\pm 7.0^\circ$ for 1.0 s (Dwell Time: 1000 ms) or when failed to dwell on the menu item within 5.0 s; in either case, the central menu item was generated. The same procedure was then repeated for the next menu item.

During the main sessions, participants engaged in a total of 15 sessions. They were assigned a $iDistance$ for each session comprising 8 trials, each associated with a different $iDirection$. One trial entailed one task, and the users experienced one $iDistance$ session 3 times. Once those three sessions were completed, they were asked to fill out the physical comfort, mental comfort, and NASA-TLX questionnaire. This procedure was repeated 5 times, associated with the $iDistance$ values. After completing all 15 sessions, participants were asked to complete a questionnaire on the entire study. The study took approximately 30 min.

3.5 Data Collection and Preprocessing

All gaze points were recorded as a point from the origin and a vector in the direction of the gaze ray. We extracted the data in two ways [10]. First, when the participant succeeded in the menu item selection, the gaze data was stored for 0.8 s, excluding the first 0.2 s of the 1.0 s allotted for menu item selection. Next, when the

participant failed to select the menu item, we recorded all gaze data for 5.0 s and selected a 0.8 s window during which, on average, the gaze points were closest to the menu item. This postprocessing was required for 7.7% of the fixations.

For each fixation, gaze data could have been unavailable due to blinking or inadequate eye tracking. If this was confirmed for 0.1 s out of 0.8 s, we excluded this fixation from the analysis. As a result, we excluded 1.1% of the fixations. The analyzed dataset comprised a total of 1,178 fixations. The gaze ray was transcribed into a two-dimensional plane perpendicular to the straight line connecting the participant’s head and the menu item (Figure 3) (b), referring to [64].

4 RESULT #1

We used a nonparametric aligned ranks transformation (ART) method [17, 45, 61] to evaluate the error rate, physical comfort and mental comfort. We conducted a Shapiro-Wilk test for all datasets and confirmed that all datasets were not normally distributed. Then, the results were analyzed using a mixed-effects restricted maximum likelihood (REML) model. The within-factor post-hoc analyses were done using pairwise Tukey-corrected least-squares means. Cross-factor pair-wise comparisons were performed using Wilcoxon signed rank tests with Holm correction [19] for the NASA-TLX data. The comprehensive results consist of a long list of datasets; please see the supplemental material for full details. Here we only present the key findings of the study.

4.1 Error Rate, Physical Comfort, and Mental Comfort

We observed significant effects and interactions on the error rate, physical comfort, and mental comfort caused by both independent variables $iDistance$ and $iDirection$. For $iDistance$, post-hoc pairwise comparisons revealed significant differences for all pairs on the error rate, physical comfort, and mental comfort, with the exception of $22-32^\circ$ on the error rate. For $iDirection$, because the results of multiple comparisons were very long, please see our supplemental material for the full details. Overall, for $iDirection$, we observed significant differences in all combinations of $0^\circ-45^\circ$, $0^\circ-90^\circ$, $0^\circ-135^\circ$, $45^\circ-270^\circ$, $45^\circ-315^\circ$, $90^\circ-180^\circ$, $90^\circ-225^\circ$, $90^\circ-270^\circ$, $90^\circ-315^\circ$, $135^\circ-270^\circ$, and $135^\circ-315^\circ$ on the error rate, physical comfort, and mental comfort. The results are summarized in Table 2 and 3. Figure 5 presents the error rate, physical comfort, and mental comfort dependence on both $iDistances$ and $iDirections$.

4.2 Error Rate

The results show that the larger the $iDistance$, the larger the error rate. $iDistance$ and $iDirection$ were independent variables, while the error rate was a dependent variable. We observed significant effects of $iDistance$ ($F_{4,1151} = 165.36$, $p < .01$) and $iDirection$ ($F_{7,1151} = 31.23$, $p < .01$) on error rate. Significant interactions were also observed $iDistance \times iDirection$ ($F_{28,351} = 11.59$, $p < .01$). Figure 5a presents the error rates with respect to $iDirection$ for all $iDistance$.

4.3 Physical Comfort

The results show that the larger the $iDistance$, the less the physical comfort. $iDistance$ and $iDirection$ were independent variables, while

physical comfort was a dependent variable. We observed significant effects of *iDistance* ($F_{4,351} = 111.94$, $p < .01$) and *iDirection* ($F_{7,351} = 20.18$, $p < .01$) on physical comfort. Significant interactions were also observed *iDistance* \times *iDirection* ($F_{28,351} = 2.84$, $p < .01$). Figure 5b presents physical comfort with respect to *iDirection* for all *iDistance*.

4.4 Mental Comfort

The results show that the larger the *iDistance* is, the less the mental comfort. The *iDistance* and *iDirection* were independent variables, while mental comfort was a dependent variable. We observed significant effects of *iDistance* ($F_{4,351} = 59.95$, $p < .01$) and *iDirection* ($F_{7,351} = 10.77$, $p < .01$) on mental comfort. Significant interactions were also observed *iDistance* \times *iDirection* ($F_{28,351} = 2.11$, $p < .01$). Figure 5c presents mental comfort with respect to *iDirection* for all *iDistance*.

Table 2: Results of the ART of error rate (ER), physical comfort (PC), and mental comfort (MC). All factors are significantly different ($p < .01$).

Factor	DV	df	df.res	F
<i>iDistance</i>	ER	4	1151	165.36
<i>iDirection</i>	ER	7	1151	31.23
<i>iDistance</i> \times <i>iDirection</i>	ER	28	1151	11.59
<i>iDistance</i>	PC	4	351	111.94
<i>iDirection</i>	PC	7	351	20.18
<i>iDistance</i> \times <i>iDirection</i>	PC	28	351	2.84
<i>iDistance</i>	MC	4	351	59.95
<i>iDirection</i>	MC	7	351	10.77
<i>iDistance</i> \times <i>iDirection</i>	MC	28	351	2.11

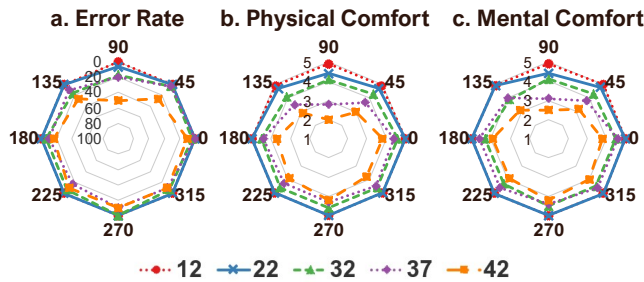


Figure 5: (a) Error rate (b) physical comfort (c) mental comfort rating for each *iDirection*. The error rate, physical comfort, and mental comfort worsened as the *iDistance* increased.

4.5 NASA Task Load Index (NASA-TLX)

The results show that the larger the *iDistance*, the larger the overall NASA-TLX workload scores. The overall NASA-TLX workload scores for each *iDistance* (12° , 22° , 32° , 37° , 42°) were 6.00, 10.90, 21.83, 35.23 and 41.87, respectively (lower is better). We performed the Friedman test on the responses to each of the six questions and the overall score, and observed significant effects on the Mental

Table 3: Average error rate (ER), physical comfort (PC), and mental comfort (MC) of each *iDistance* and *iDirection*. The error rate, physical comfort, and mental comfort of *iDirection* correspond to *iDistance* = 32° , 37° , and 42° .

	ER	PC	MC
iDistance			
12	0.0 %	4.96	4.98
22	0.8 %	4.85	4.89
32	7.5 %	4.43	4.30
37	10.0 %	3.99	4.21
42	20.0 %	3.41	3.58
iDirection			
0	4.4 %	4.20	4.30
45	11.3 %	3.65	3.77
90	28.9 %	3.05	3.23
135	17.8 %	3.50	3.67
180	4.4 %	4.10	4.27
225	11.1 %	4.25	4.27
270	11.1 %	4.40	4.37
315	8.9 %	4.20	4.37

Table 4: Error rate for each *iDistance* and *iDirection*.

	iDistance				
	12	22	32	37	42
iDirection					
0	0.0 %	0.0 %	3.3 %	0.0 %	10.0 %
45	0.0 %	0.0 %	3.3 %	3.3 %	26.7 %
90	0.0 %	6.7 %	16.7 %	20.0 %	50.0 %
135	0.0 %	0.0 %	16.7 %	10.0 %	26.7 %
180	0.0 %	0.0 %	6.7 %	10.0 %	16.7 %
225	0.0 %	0.0 %	6.7 %	16.7 %	10.0 %
270	0.0 %	0.0 %	0.0 %	10.0 %	10.0 %
315	0.0 %	0.0 %	6.7 %	10.0 %	10.0 %
avg.	0.0 %	0.8 %	7.5 %	10.0 %	20.0 %

($\chi^2_{4,N=10} = 23.33$, $p < .01$), Physical ($\chi^2_{4,N=10} = 31.01$, $p < .01$), Temporal ($\chi^2_{4,N=10} = 16.98$, $p < .01$), Performance ($\chi^2_{4,N=10} = 22.88$, $p < .01$), Effort ($\chi^2_{4,N=10} = 29.80$, $p < .01$), Frustration ($\chi^2_{4,N=10} = 18.62$, $p < .01$), and overall workload ($\chi^2_{4,N=10} = 30.67$, $p < .01$) for *iDistance*. Figure 6 shows NASA-TLX scores by *iDirections* for all *iDistances*.

4.6 The Menu Item Size required to enable Robust Interaction in the Kuiper Belt

The higher error rate in menu item selection when the menu item moves away from the center of vision indicates that the menu item size needs to be changed to maintain the same error rate and achieve robust interaction as it moves away. We compute the sphere diameter required to enable robust interaction in the Kuiper Belt for all gaze points during menu item fixation. Table 5 shows the resulting sphere diameters computed based on the overall menu item fixations and over different percentiles of users for each *iDistance* and *iDirection*. This parameter will be used in Study #2.

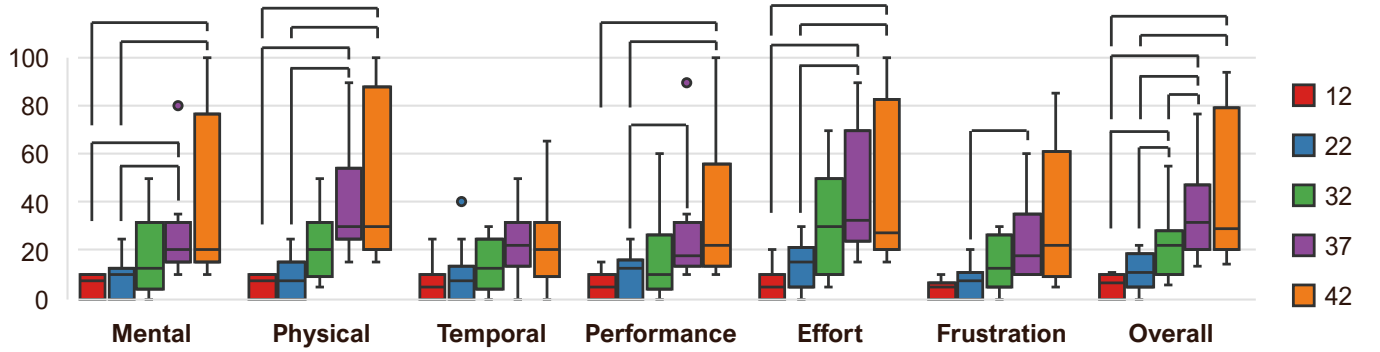


Figure 6: Responses to the NASA-TLX questionnaires. Error bars are standard errors. All statistically significant differences are at $p < .05$.

Table 5: Recommended sphere diameter ($^{\circ}$) for robust and smooth interaction by eye gaze for each $iDistance$ or $iDirection$.

	Inclusion Percentile			
	25%	50%	75%	90%
$iDistance$				
12	1.40	2.33	3.72	5.20
22	2.58	3.89	5.84	7.82
32	2.90	4.83	7.45	11.68
37	3.09	5.25	8.54	12.02
42	4.15	7.17	11.12	16.27
$iDirection$				
0	2.03	3.69	6.13	9.12
45	2.90	4.75	7.60	11.27
90	2.78	5.22	10.12	14.71
135	3.37	5.36	8.39	11.70
180	2.46	4.89	7.75	11.79
225	2.57	4.24	7.05	11.75
270	1.87	3.18	5.37	8.25
315	2.30	3.71	6.26	8.77

4.7 Summary of Study #1

We implemented the Kuiper Belt in the VR environment. The error rate of the range for $iDistance = 32^{\circ}$ and 37° , which is the out-of-natural angle region, was less than 10% (min = 0% at $iDistance = 32^{\circ}$, $iDirection = 0^{\circ}$ and 270° . Max = 20% at $iDistance = 37^{\circ}$, $iDirection = 90^{\circ}$). On the other hand, the overall error rate at $iDistance = 37^{\circ}$ was 20%, which presents difficulties in practice; therefore, the region of $iDistance = 32^{\circ}$ and 37° is a candidate for the Kuiper Belt in the VR environment. However, the overall results of the experiment showed that the greater the $iDistance$, the worse the error rate, physical comfort, and mental comfort. In particular, the fatigue increased significantly for upward menu item selection, and a 50% error rate was recorded for pointing directly above when $iDistance = 42^{\circ}$ at $iDirection = 90^{\circ}$. The gaze distribution of all gaze points during a menu item fixation was elongated in relation to the menu item direction, and the accuracy and precision worsened as $iDistance$ increased. The results are consistent with those suggested

by Tobii’s internal experiments¹. Therefore, for menu items placed in the Kuiper Belt to include as much of the gaze data as possible, a large menu item size is needed.

Again, the experimental results showed that physical comfort, mental comfort, and error rate worsened as $iDistance$ increased. We speculate that this is because the closer the menu item position to the limit of the human eye movement, the more the effort required to move the eyes. In particular, the worsening of the indicators was marked by upward menu item placement (top, right, and left). We can assume that this is because the FOV is narrower upwards than downwards. Therefore, it is preferable to place the menu item in the horizontal or downward direction, which means that the Kuiper Belt in VR is not a perfect circle, but a distorted circle. As a result, in the cases of $iDirection = 45^{\circ}, 90^{\circ}, 135^{\circ}$ and $iDistance = 32^{\circ}, 37^{\circ}$ are the acceptable regions, and in the case of $iDirection = 180^{\circ}-360^{\circ} (0^{\circ})$, $iDistance = 32^{\circ}, 37^{\circ}, 42^{\circ}$ are the acceptable regions for interaction.

5 STUDY #2: MEASURING THE EFFICIENCY OF THE KUIPER BELT MENU ITEM PLACEMENT METHOD

We conducted a second study to investigate whether the Kuiper belt method is effective in solving the Midas touch problem for the menu item selection task and the visual search task, where the Midas touch problem (false input) is frequently encountered. In this study, we compare the Kuiper Belt-based menu-selection method with the other two methods: the two-step gaze-selection and the head-gaze methods. The overall study setup for study #2 is the same as that of study #1. This study was conducted in January and February of 2021.

5.1 Participants

Nineteen participants were enrolled, but one was eliminated because of calibration error. Hence, we used data from 18 participants (Three female, mean age 22.7 years, SD = 1.7 years) for our analysis. All had normal or corrected-to-normal vision, and one had prior experience with an eye-tracking interface. No participants wore eyeglasses; as in study #1, we utilized the unnatural region of the eye gaze where the eye tracker cannot track the gaze of a person

wearing eyeglasses. Each participant received a US\$ 10 gift voucher, and each study took approximately 60 min.

5.2 Methods for comparison

We compare three eye-gaze-based menu-selection methods: two-step selection (2SS), head gaze (HG), and head gaze with Kuiper Belt (KB). Figure 7 illustrates the three methods and the user's perspective of each method. The task of this study is a visual search task, in which a user is asked to search a 3D scene visually to find and select a target panel on a square plate, and then select an item in a menu displayed in the 3D world. The positions of items in the menu are arranged in the same eight directions as those in Study #1.

5.2.1 Two-step selection method (2SS). The 2SS is the baseline for the gaze-based menu-selection method. The baseline was evaluated on A) a two-step method, B) dwell-time based method, C) selectable targets placed in the visual search space, and D) circular menu method similar to the KB/HG method. 2SS satisfied all and thus was found reasonable for the comparison.

The operation of the 2SS method is summarized in the following two steps:

- (1) The user selects a target panel by looking at it for X ms, where X is an independent variable defined by the study design.
- (2) After the user selects a target panel, the menu items are displayed in the user's line-of-sight position and are fixed in the 3D world. The user selects an item in the menu by looking at the item for X ms, where X is an independent variable defined by the study design.

Target panels and menu items are selected using a dwell time-based selection method. The dwell time is the same for both target panel and menu-item selection. The dwell time is an independent variable. Menu items were placed at $iDistance = 12^\circ$. The diameter of the 2SS menu items is 5.2° . This size is sufficient for robust and smooth eye-gaze selection in the case of $iDistance = 12^\circ$, according to study #1 (Table 5).

5.2.2 Head-gaze method (HG). We designed two head-gaze methods; one is HG, wherein menu items are placed within the natural range of eye movement (12°), and the other method, KB, places the menu items in the Kuiper Belt. HG involves simultaneous application of target panel and menu item selection. The operation of this method is summarized in the following two steps:

- (1) The user turns his/her head toward the target.
- (2) The user selects an item in the menu by looking at the item for X ms, where X is an independent variable defined by the study design, while the user's head remains pointing at the target panel.

Unlike 2SS, the user first intercepts the target panel via head movement, and then selects the menu item via eye gaze. HG accomplishes target panel and menu item selection separately by using a simultaneous two-point technique. The HG menu is fixed to HMD and placed within natural head-eye angles ($iDistance = 12^\circ$). The diameter of the HG menu items is 5.2° , which is the same as that of 2SS.

5.2.3 Head gaze with Kuiper Belt method (KB). The menu item selection method of KB is the same as that of HG; only the location of the menu items and the menu region are different. The $iDistance$ of the KB menu is positioned at 32° in the upward direction ($iDirection = 45$ to 135°) and 37° in the other $iDirections$, based on the results of Study #1. The diameter of the KB menu items is 12° . This size is sufficient to achieve robust and smooth eye-gaze selection in case of $iDistance = 37^\circ$, according to study #1 (Table 5). So, the absolute size of the menu item of KB is larger than that of 2SS and HG, but the difficulty of eye-gaze selection is the same as that of 2SS and HG.

5.3 Design

We used a within-participant design. The two independent variables were as follows:

- Method (2SS, HG, KB)
- Dwell time (DT ; 200, 400, 600 ms)

The number of menu items is 8, and the items are placed at the same angle as the $iDirection$ in Study #1. The items in the menu are spheres with colors selected from ColorBrewer². We choose set 1, which includes 8 colors (green, blue, red, pink, gray, yellow, orange, and purple) that are assigned to each of the 8 $iDirections$ (0° , 45° , 90° , 135° , 180° , 225° , 270° , 315°).

In the eye-gaze interface, 600 ms is the standard *dwell time* (DT) [66]; many existing interfaces employ this value (e.g., [33]). We selected shorter DT values (200 ms and 400 ms), as these cause the Midas touch problem more frequently than the standard used in visual search and menu item selection tasks.

The order of the *method* was counterbalanced using a Latin square. Participants underwent 2 sessions \times 16 trials (8 directions of study #1 \times 2) for each DT , using each *Method*. The order of the DT was counterbalanced using a Latin square. Finally, we collected 3 *Methods* \times 3 DT s \times 2 times \times 16 trials (8 directions of study #1 \times 2) = 288 valid menu-item-selection datasets for each participant (5,184 datasets in total).

The main dependent variables were trial time and error rate. If a wrong target panel or menu item was selected, the task was considered erroneous. We employed System Usability Scale (SUS) [4] and NASA-TLX [15] questionnaires to measure usability and workload in terms of user strain for each *Method*. In addition, all participants completed a questionnaire to indicate their preference for dwell time and method.

5.4 Procedure and Task

All equipment and material touched by the participants were disinfected before the experiment. The hands of the experimenter and staff were sanitized, as well. First, we welcomed the participants and asked them to sanitize their hands and briefly introduced them to the study. All participants provided written and informed consent. We provided detailed task instructions using graphical images. The participants performed 5-point eye-tracking calibration of initially installed software on the HTC Vive Pro Eye. All participants engaged in a practice session before the main sessions started; different parameters were used for the practice session.

²<https://colorbrewer2.org/#type=qualitative&scheme=Set1&n=9>

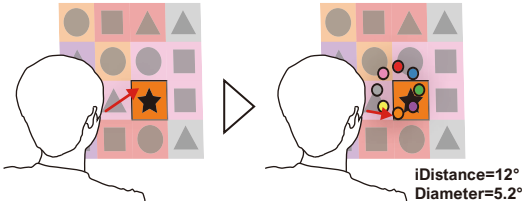
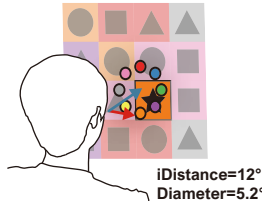
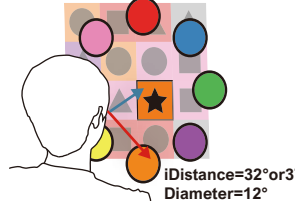


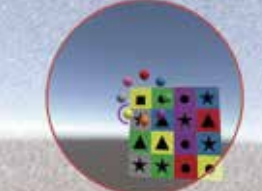
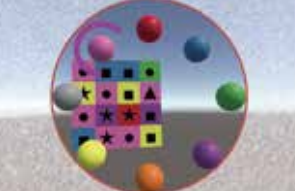
	Two-step Selection (2SS)	Head-Gaze (HG)	Head-Gaze with Kuiper Belt (KB)
Method	<p>1. Panel selection with gaze 2. Menu item selection with gaze</p>  <p>iDistance=12° Diameter=5.2°</p>	<p>Panel selection with head direction and menu item selection with gaze</p>  <p>iDistance=12° Diameter=5.2°</p>	<p>Panel selection with head direction and menu item selection with gaze</p>  <p>iDistance=32° or 37° Diameter=12°</p>
Camera View	 		

Figure 7: Brief overview of the three methods and the corresponding FOVs. The red circle in the camera view represents the FOV.

The task was a visual search task, wherein we asked the participants to find and select a panel (target) and color (menu item) with the eye-gaze interface in a VR environment. Each plate consisted of 4×4 16 panels, placed 2.0 m from the participant’s head and had a width and height of 50° . Each participant was asked to find and select a target panel from a plate and then select the target color of the panel from the menu items. Colors were assigned randomly to each panel, and each panel had a symbol (a circle, square, triangle, or star). The target panel shows a symbol that appears on that panel only; the other 15 panels show one of the three other symbols. The task for the participants was to find and select a panel that displays a symbol only once among 16 panels, and to also select the color of the target panel from the 8 color items in the menu displayed in the 3D world. The 2SS menu was displayed after selecting a panel, and the HG and KB menus were always displayed. The menu was placed at a depth of 1.8 m from the HMD. All trials were performed sequentially, and when the correct target and color were selected, the panels were regenerated. When a selection error occurred, the plate was regenerated after pausing for 500 ms to prevent successive errors. To solve the Midas touch problem, the 200 ms right after the completion of the trial was not included in the dwell time. As feedback, a sound corresponding to a correct or incorrect answer was played when the target was selected.

The currently selected panel was highlighted, and the same circular slider feedback of study #1 was displayed when gazing at the item in the menu. A head cursor was displayed when using HG and KB, and a gaze cursor was displayed when using 2SS. The diameters of the head and gaze cursors were 1.0° . We applied an outlier filter [25] with a Gaussian kernel [24] to the gaze data.

During the study, participants experienced 18 sessions in total. First, they were assigned a *Method* and then a *DT*. One session consists of 8 tasks associated with the *iDirections* of Study #1 \times 2; so one session has 16 tasks. The participants experienced one combination of *Method* \times *DT* for 2 times. Once a participant experienced all 3 *DT*

for *Method* (so one *Method* has 6 sessions in total), they were asked to fill out the SUS, NASA-TLX, and dwell-time preference questionnaires. This procedure was repeated 3 times, associated with the *Methods*. After completing all 18 sessions, participants were asked to indicate their method of preference and were interviewed. The study took 60 min to complete.

6 RESULT #2

We used a nonparametric ART method [17, 45, 61] to evaluate the trial time and error rate because we conducted a Shapiro-Wilk test for all datasets and confirmed that all datasets were not normally distributed. Then, the results were analyzed using a mixed-effects REML model. The within-factor post-hoc analyses were performed using pairwise Tukey-corrected least-squares means. Cross-factor pair-wise comparisons were done using Wilcoxon signed rank tests with Holm correction and applied to the SUS and NASA-TLX. The comprehensive results include a long list of datasets; please see the supplemental material for full details. Here we present key findings of the study.

6.1 Trial Time

The results show that the larger the *Dwell time* (*DT*), the larger the trial time. The *Method* and *Dwell time* (*DT*) served as independent variables, and the trial time was a dependent variable. We found the significant main effects of *Method* ($F_{2,4032.4}=9.70$, $p<.01$), and *DT* ($F_{2,4032.5}=75.04$, $p<.01$). We noted significant interactions: *Method* \times *DT* ($F_{4,4032.0}=11.61$, $p<.01$). Post-hoc tests revealed significant differences between 2SS and KB ($Z=3.57$, $p<.01$) in the trial time under the condition of *DT* = 600 ms. Figure 8 and Table 6 display trial time by *DT* values for all *Methods*.

6.2 Error Rate

The results show that HG and KB had significantly lower error rates than 2SS for all DT values. The *Method* and *Dwell time (DT)* served as independent variables, and the error rate was a dependent variable. We found significant main effects of Method ($F_{2,5158}=2321.23$, $p<.01$), and DT ($F_{2,5158}=2519.50$, $p<.01$). We noted significant interactions: Method \times DT ($F_{4,5158}=571.56$, $p<.01$). Post-hoc tests revealed significant differences between 2SS and HG ($Z = 18.11$, $p < .01$), 2SS and KB ($Z = 21.52$, $p < .01$), and HG and KB ($Z = 9.14$, $p < .01$) in the error rate under the condition of DT=200 ms. For the case of DT=400 ms, post-hoc tests revealed significant differences between 2SS and HG ($Z = 11.12$, $p < .01$), 2SS and KB ($Z = 12.86$, $p < .01$), and HG and KB ($Z = 3.58$, $p < .01$) in the error rate. For the case of DT=600 ms, post-hoc tests revealed significant differences between 2SS and HG ($Z = 6.58$, $p < .01$), 2SS and KB ($Z = 4.61$, $p < .01$), and HG and KB ($Z = -2.33$, $p < .05$) in the error rate. Figure 8 and Table 6 display error rate by DT values for all Methods.

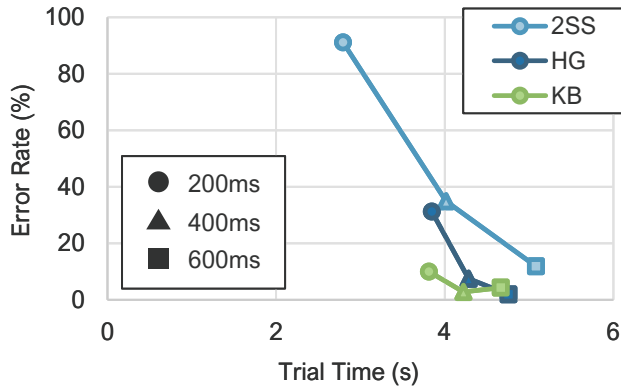


Figure 8: Trial time \times error rate by DT.

Table 6: Median of trial time and error rate by *Method* \times *DT*.

		Dwell Time		
		200 ms	400 ms	600 ms
2SS	Trial Time	2.79 s	4.01 s	5.05 s
	Error Rate	91.15 %	34.90 %	11.81 %
HG	Trial Time	3.85 s	4.29 s	4.76 s
	Error Rate	31.25 %	7.47 %	1.91 %
KB	Trial Time	3.81 s	4.23 s	4.67 s
	Error Rate	10.07 %	2.78 %	4.34 %

6.2.1 Analyzing the Midas touch for 2SS. There are two types of errors when using 2SS: errors when selecting panels (Midas touch during visual search) and errors when selecting menu items (Midas touch during menu item selection). The errors when selecting menu items for 2SS was 1.39% when DT=200, 0.52% when DT=400, and 0.17% when DT=600, which are quite small compared to the overall error rate in 2SS. Therefore, most of the errors by 2SS are Midas touches during visual search.

6.2.2 Analyzing the Midas touch for HG and KB. There are also two types of errors when using HG and KB, but the errors are different than those of 2SS. The task in Study #2 is a visual search task in which a user was asked to find and select a correct panel. So, in certain cases the participants selected an incorrect panel but they thought it was correct. This error is not the Midas touch error because it is intentional so we excluded it, for example, the error of selecting a panel as the target while the selected panel is incorrect. In another case, the user successfully selected a menu item for the menu item selection task, but it was the incorrect item. We define this error as a visual search error. We excluded this error from Midas touch, as well, because it is an intentional menu item selection by the user, which is successful albeit incorrect. We defined all other errors as Midas touch in HG and KB.

We used a nonparametric ART method [17, 45, 61] using a mixed-effects REML model to evaluate the visual search error rate and error rate. The within-factor post-hoc analyses were performed using pairwise Tukey-corrected least-squares means. Cross-factor pair-wise comparisons were done using Wilcoxon signed rank tests with Holm correction.

The results showed there was no significant difference in all combinations for the visual search error rate. The *Method* and *Dwell time (DT)* served as independent variables, and the visual search error rate was a dependent variable. We found significant main effects of Method ($F_{1,3433}=261.89$, $p<.01$), and DT ($F_{2,3433}=5.47$, $p<.01$). We noted significant interactions: Method \times DT ($F_{2,3433}=268.20$, $p<.01$).

The results show that KB exhibited a significantly lower Midas touch rate than HG, except for the 600 ms sample. The *Method* and *Dwell time (DT)* served as independent variables, and the Midas touch rate was a dependent variable. We found significant main effects of Method ($F_{1,3433}=1406.06$, $p<.01$), and DT ($F_{2,3433}=185.45$, $p<.01$). We noted significant interactions: Method \times DT ($F_{2,3433}=370.66$, $p<.01$). Post-hoc tests revealed significant differences between HG and KB ($Z = -9.19$, $p < .01$) in the Midas touch rate under the condition of DT=200 ms. For the case of DT=400 ms, post-hoc tests revealed significant differences between HG and KB ($Z = -4.00$, $p < .01$) in the Midas touch rate. For the case of DT=600 ms, post-hoc tests revealed significant differences between HG and KB ($Z = 2.71$, $p < .05$) in the Midas touch rate.

The Midas touch rate was classified for only HG and KB, because 2SS cannot discriminate between visual search errors. Figure 9 and Table 7 display the visual search error rate and Midas touch rate by DT values for HG and KB.

Table 7: The visual search error rate and the Midas touch rate by *Method* \times *DT*.

Method		Dwell Time		
		200 ms	400 ms	600 ms
HG	Search Error	4.69 %	2.60 %	1.74 %
	Midas Touch	26.56 %	4.87 %	0.17 %
KB	Search Error	3.30 %	1.91 %	2.60 %
	Midas Touch	6.77 %	0.87 %	1.74 %

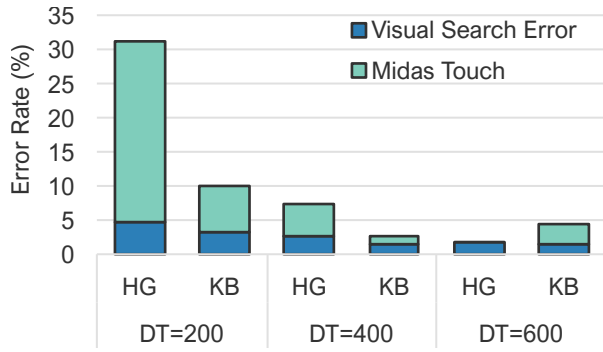


Figure 9: The visual search error rate and the Midas touch rate by DT.

6.3 System Usability Scale (SUS)

The overall SUS scores for each *Method* (2SS, HG, KB) were 49.44, 69.31 and 71.94, respectively (higher is better). We performed the Friedman test on the overall scores. The overall SUS score was significant ($\chi^2_{2,N=18} = 17.77$, $p < .01$) for Method. Post-hoc tests revealed significant differences between 2SS and HG ($Z = -3.34$, $p < .01$), and 2SS and KB ($Z = -3.60$, $p < .01$) in the overall SUS score. Figure 10 (a) presents the SUS scores of all Methods.

6.4 NASA Task Load Index (NASA-TLX)

The overall NASA-TLX workload scores for each *Method* (2SS, HG, KB) were 62.85, 46.28 and 37.91, respectively (lower is better). We performed the Friedman test on the responses for each of the six questions and the overall score. The Method was significantly affected by Mental ($\chi^2_{2,N=18} = 16.60$, $p < .01$), Temporal ($\chi^2_{2,N=18} = 23.43$, $p < .01$), Performance ($\chi^2_{2,N=18} = 23.91$, $p < .01$), Effort ($\chi^2_{2,N=18} = 10.64$, $p < .01$), Frustration ($\chi^2_{2,N=18} = 9.76$, $p < .01$), and overall workload ($\chi^2_{2,N=18} = 12.76$, $p < .01$). Post-hoc tests revealed significant differences between 2SS and HG ($Z = 2.85$, $p < .01$), and 2SS and KB ($Z = 3.34$, $p < .01$) in the overall NASA-TLX workload score. Figure 10 (b) presents the NASA-TLX scores for all Methods.

6.5 Dwell-Time Preference

Figure 11 (a) displays the results of participant preference for *DT*. From the figure, the most favorable dwell time is 600 ms for 2SS, 400 ms or 600 ms for HG, and 200 ms or 400 ms for KB.

The KB dwell time of 200 ms or less, which is too short for a normal gaze interface, was preferred by 9 participants. Participant P12 commented “*Since there were almost no unintentional wrong inputs, there was no problem even if the dwell time was short.*” The HG dwell times of 400 ms or 600 ms were preferred by 14 participants. Unlike the 2SS, the participants preferred a relatively short dwell time (400 ms). P18 commented “*The dwell time of 600 ms seems long.*” In general, the participants did not like dwell times that were too short. P6 commented “*In case of dwell time is short, I moved my gaze frequently or stared only at the front to avoid false selection.*” In 2SS, 13 participants preferred a dwell time of 600 ms or more. Participants were frustrated when the dwell time was too short.

P13 commented “*When the dwell time is short, 2SS is difficult to use because there is no room to explore the panels.*”

6.6 Method Preference

Figure 11 (b) displays the Method of preference of the participants, namely KB, HG, and 2SS, in that order. KB was rated as the most preferred by 9 participants, HG by 5 participants, and 2SS by 4 participants. The average ranks for KB, HG, and 2SS were 1.44, 2.00, and 2.44, respectively.

KB was the most preferred method, with 17 participants rating it as the first or second most preferred method. P13 commented “*The menu items were far away, so there was no time pressure at all, regardless of the dwell time.*” However, participants reported that a menu item was selected multiple times when the dwell time was short. P14 commented “*Since the system moves to the next trial immediately after the menu item is selected, the same menu item was selected consecutively when the dwell time was 200 ms.*” We did not count the 200 ms as dwell time immediately after the completion of a trial to avoid the (another) Midas touch, but this value seems to be too small to prevent unintended selection. It should be a larger value (e.g., 300 ms or 400 ms) to address this issue.

HG was the second most preferred method, with 13 people rating it as the first or second most preferred method. P18 commented “*Head cursor was easy to do.*” However, participants reported that the menu items at the center of the field of view were distracting. P11 commented “*The panels were hidden by menu items, so it was hard to see.*” P14 commented “*I tried to keep my eyes away from the menu items to avoid selection errors.*”

2SS was the least preferred method, with 12 participants rating it their third most preferred method because of its high error rate due to the short dwell time. P17 commented “*When the dwell time was too short, the selection was completed before I could recognize the panel.*” On the other hand, there were some people who rated 2SS as the best because of the advantage of not having to move their head significantly. P9 commented “*2SS was easy because I hardly had to move my head.*”

6.7 Summary of Study #2

The Kuiper Belt (KB) menu item placement method can reduce error rate (false input as the Midas touch) in menu item selection and visual search task. Although 2SS was the fastest method, the error rate was too high (91.15%@200 ms and 34.90%@400 ms) to be of practical use. HG was accurate at DT = 400 ms and 600 ms, but had a large error rate at DT = 200 ms (31.25%). Similarly, the mean scores for usability and workload were better for KB, HG, and 2SS, in that order. KB and HG had significantly better usability and workload scores than 2SS. All in all, the Kuiper Belt method was stable toward the variance of dwell time. Although refinements will be necessary for practical usage, the error rate was adequately low for a first research prototype. Thus, it is concluded that the Kuiper Belt method can reduce the false inputs.

KB was the most accurate and generated significantly less time pressure than the other methods. KB was better than 2SS in terms of error rate, usability, and workload. In addition, KB had a significantly lower error rate than HG at a DT of 200 ms. The mental demand, temporal demand, and performance of the NASA-TLX

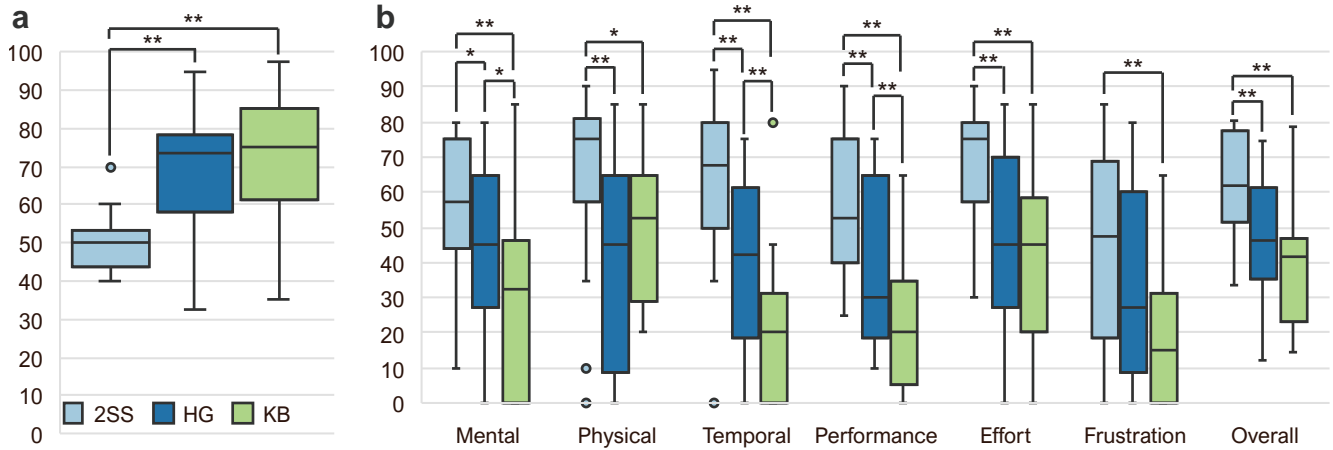


Figure 10: Responses to the (a) SUS and (b) NASA-TLX questionnaires. The error bars are standard errors. Statistical significance: * $p < .05$, ** $p < .01$.

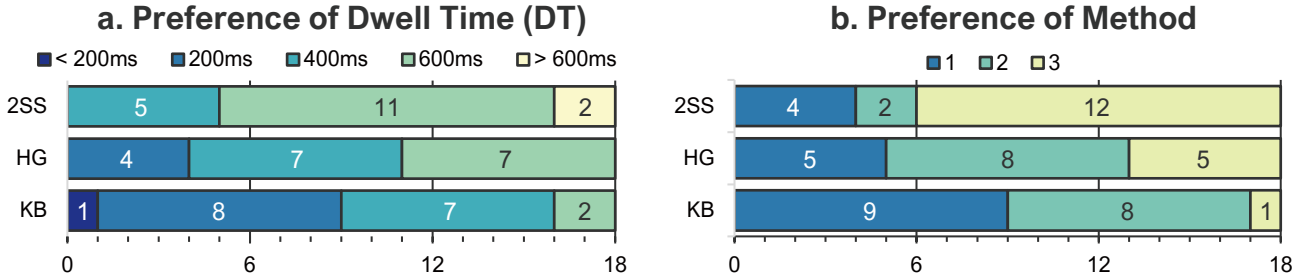


Figure 11: The results of user preference for (a) dwell time and (b) method.

item were significantly better than those of HG. Hence, KB is more suitable for the visual search task than the other two methods.

HG was better than 2SS in terms of error rate, usability, and workload. Furthermore, it was able to reduce the Midas touch at a dwell time of 400 ms. Therefore, HG is a better method for visibility search tasks than 2SS. Finally, 2SS had a very high error rate, necessitating the use of dwell times of greater than 600 ms. This is consistent with previous studies [66] indicating that the required dwell time is longer in high-workload tasks. Increasing the dwell time to reduce false selection leads to an increase in selection time. Hence, 2SS is more suitable for short and simple operations rather than visual search tasks.

7 EXAMPLE APPLICATIONS

Here, we show four example applications illustrating our findings from the user study. These applications are just mock-ups.

7.1 Application Menus and Control with Kuiper Belt

The primary usage of the Kuiper Belt method is for menu-item selection. The results of Study #2 show that the use of the Kuiper Belt can reduce Midas touch during visual search. Because visual search tasks are a common task in the VR environment, applications

using Kuiper Belt are effective to improve the user experience in the VR with an HMD. This example displays an application menu (Figure 12a). The menu items are placed outside the FOV while users are looking toward the front to avoid interference with the view. Once the user's gaze enters the Kuiper Belt, the menu items move smoothly into the Kuiper Belt, the design of which is inspired by the Gaze-Summon interface [30]. The arrangement of these menu items and controls are not frequently changed so that the user can easily memorize the icon locations. This contributes to effective control, and users can use the Kuiper Belt interface smoothly and accurately while reducing the false input (Midas touch problem).

7.2 Eye-Gaze Interface for Home Appliances in VR

The second example is a remote for controlling home appliances in VR (Figure 12b). The remote use is similar to the tasks in Study #2; the user first selects a target appliance with the head direction, and the menu items are then displayed around the FOV. The menu items are placed in the Kuiper Belt zone to reduce the false input (Midas touch problem). This example illustrates that the user can control home appliances only with a gaze interface, realizing a fully hands-free interaction. We expect that this prototype will also work

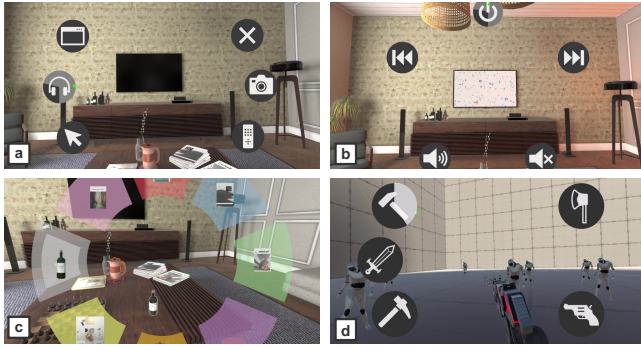


Figure 12: Illustration of application with Kuiper Belt. The green dot is the user’s line of sight. a) Main menu. b) Trying to turn off the TV. c) Selecting a bottle. d) Holding a gun.

in the MR environment, e.g., actual home appliance control with Microsoft Hololens 2 with the eye-tracking interface.

7.3 Selecting a Small and Dense Object from a Group of Objects

The third example demonstrate an object selection from a group of objects and manipulating a target object. In a 3D environment, it is challenging to select an object if it overlaps with other things or if the object is too small visually. We designed a method to address this problem (Figure 12c), which was inspired by Actigaze [31], a method to select a small and dense object by gaze only. From the results of Study #2, the gaze interaction area and the visual search area can be separated by placing the menu icon in the Kuiper Belt, similar to ActiGaze. While Actigaze is designed for the GUI (2D) environment, we have developed an extension of this method for VR. When a user looks at a group of objects, which has a target object to be selected, each object will be highlighted with colors associated with menu items on the Kuiper Belt. The selection is then completed by selecting a menu item placed in the Kuiper Belt that has the same color as the target object. This application makes it easy to select an object that is difficult to select by direct gaze pointing.

7.4 Items Selection in VR Games

The Kuiper Belt can also be used in VR games. The results of Study #2 show that the Kuiper Belt method was sufficiently accurate to select menu items with a shorter dwell time. This example demonstrates that the user can select an item in a game with the eye-gaze interface (Figure 12d). The users may have controllers in their hands while they are gaming in VR, which is acceptable because the eye-gaze interface can be used to complement other interfaces. We take advantage of the users’ natural behavior; they look at the items on the menu list when they want to change items. With the Kuiper Belt interface, the user can select an item just by looking at the item on the menu because it is included in the eye-gaze interface. The Kuiper Belt supports this type of natural behavior and can work with existing interfaces, such as game controllers and gestural interfaces.

8 DISCUSSION

We conducted two studies to investigate whether the Midas touch problem could be reduced by placing selectable items on the Kuiper Belt (KB). The KB method is an eye-gaze-based interface design principle, whereby the target items in the menu are placed in the out-of-natural angle region of the eye-gaze movement. Here, we summarize our two studies.

- **Study #1:** We investigated where menu items should be placed in the Kuiper Belt and determined that the items should be placed at $iDistance = 32^\circ$ and 37° in the upward direction and at $iDistance = 32^\circ$, 37° , and 42° in the downward direction.
- **Study #2:** The KB method was evaluated and found to be an accurate method that worked well even with a short dwell time (200 ms). The workload of the KB method was the lowest among the three methods, especially in terms of mental demand, temporal demand, and performance. The Kuiper Belt menu-selection method utilized the out-of-natural angle region of the eye-gaze movement at a similar level of workload as that of an interface designed to work within the comfort zone.

The results of the error rate demonstrate that the KB method can reduce the Midas Touch problem in the visual search task. It should also be noted that the only case where KB was worse than HG was for $DT = 600$ ms. We carefully analyzed the collected data and found that one participant made frequent mistakes in KB under the first condition (method) of the study. We are not sure whether the participant understood the task correctly. Nevertheless, we did not consider this as an outlier case to be eliminated, and hence, we kept this data in our dataset. The other 17 participants worked well with the KB method. Overall, we conclude that KB is a promising method for reducing the Midas touch problem.

The level of physical demand (or user strain) and other workload indices exhibited a tendency similar to that of the interface within the comfort zone of the eye-gaze movement. Overall, we consider the Kuiper Belt menu selection method to work well for the visual search task. However, we do not claim that the Kuiper Belt is the only method to solve the Midas touch problem. Because this method utilizes the out-of-natural angle region in the eye-gaze interaction, it can work with other interaction techniques. Therefore, this method fully complements other interaction techniques.

8.1 The Applicability, Strengths, Weaknesses of the Kuiper Belt

Although we have explored the effectiveness of the Kuiper belt method on the visual search task, this method can be applicable for other VR tasks. First of all, the Kuiper Belt method is designed as a menu item selection method in VR, so it would be effective for this purpose (Example application a/b). From the results of our studies, the Kuiper Belt method was evaluated as a fast eye gaze-based menu item selection method with a reduced Midas touch, which realizes immediate access to menu items. Likewise, it would be usable for the object selection task, even though small and dense objects can be selected with the gaze alone (Example application c). Furthermore, as the eye-gaze movement was not observable from outside of the HMD, the Kuiper Belt method can be applicable

for a secret code input task, such as an unlocking interface for an HMD-based VR application.

However, the Kuiper Belt is not a general-purpose design principle and cannot be used for all tasks in VR. It is difficult to place many menu items to be selected (e.g., eye typing) in the region of the Kuiper Belt owing to the low gaze accuracy and precision of the method. It is not suitable for tasks that do not involve selection (e.g., information consumption interface). Looking at the region of the Kuiper Belt for a long time might cause fatigue from use. Likewise, tasks for which looking at the center area of vision is important for users (e.g., zooming in/out on a map application) are not suitable because users' attention needs to stay in the application window to continuously check the results of their operations. Overall, there are various operations and tasks in VR environments, the menu item selection task is an essential task in the VR with HMDs as well as the other type of computing devices (PC, mobile, tablet, etc.). The Kuiper Belt-base menu item selection method is expected to contribute to an increase in the productivity of workers who use an eye-gaze interface in a VR environment.

8.2 User Strain Using the Kuiper Belt

We conducted Study #2 to evaluate the user strain resulting from the "Out-of-natural angle" region in the eye-gaze movement. A factor that may cause user strain is moving the eyes to a high eccentricity. So, we investigated the extent to which high eccentricity causes a burden on the user by comparing the method with menu items placed in regions with both high (KB) and low (HG) eccentricity. The results of Study #2 showed that HG and KB scores were significantly better than those of 2SS in the physical demand section of NASA-TLX. In addition, there was no significant difference between HG and KB with respect to physical demand of NASA-TLX. Therefore, physical fatigue caused by the Kuiper Belt is acceptable for short-term use.

However, the user strain associated with the long-term use of the Kuiper Belt was not investigated. Sidenmark *et al.* [50] indicated that while it is possible to place UI elements out of the visibility range of the average user, it may cause long-term strain on the user. Based on Study #2, we confirmed that users could use the Kuiper Belt eye-gaze interface for about 15 minutes (96 tasks), but the effects of the additional use of this method were not investigated. Further research is required to evaluate the effect of long-term strain on users. This is a limitation of the current study.

8.3 Where Should Menu Items be placed for the Eye-gaze Interface?

The results of study #2 indicate that HG and KB are suitable for the visual search task. However, HG users are always forced to display unnatural visual search behavior to account for false selection (study #2, Participant P12: *"I tried to move my head and body as much as possible while keeping my line of sight straight, because there was a possibility that the color selection would be made by mistake if I looked in a direction other than the head direction"*), which implies that the menu displayed within the user's comfort area could block the user's line of sight in the VR environment. Similarly, the menu items selected by HG method always blocked part of the central vision because virtual content (e.g., menu and

its items) may block other objects in the 3D world. Thus it is not recommended that these items be placed in the central FOV [28]. HG can be used for short-term operations and may be hard to use for interfaces that are continuously displayed.

By contrast, the KB method displays menu items outside the central vision. It does not block any information or objects in the 3D world that the user may want to look at. It is thus easier to display menu items for a longer period of time than when displaying the menu within the central vision area. There are design spaces where the menu can be continuously displayed; menu items can move in from outside the vision, like Gaze-Summon [30]. All in all, we demonstrated the new usage of the "out-of-natural angle" region of the eye-gaze movement, which is a promising area for future eye-gaze interface and interaction research.

8.4 Remaining Midas Touch Problem of Kuiper Belt Method

The results of our study demonstrate that the Kuiper Belt method reduces the Midas touch (false selection) problem, which is primarily related to unintentional input in a visual search task. However, there are remaining Midas Touch problems we may need to clarify. A mis-selection of the menu item on the Kuiper Belt can happen during the menu item selection task. In order to reduce this Midas Touch problem within the Kuiper Belt, the menu and the items have to be carefully designed on the Kuiper Belt. For example, placing only the items that the users know well, allows them to complete their selection without having to search the menu items on the Kuiper Belt. So, preferably items that are used repeatedly should be placed in the Kuiper Belt, such as shortcuts. This accelerates the selection time, but there should be tasks and applications that are used infrequently. It is possible to address these unfamiliar menu items that affect dwell time depending on a task and application. If a task is unfamiliar to users, the dwell time may be expected to be longer. Alternatively, if an application is frequently used by a user, the dwell time can be faster. This adaptive approach can reduce the Midas touch, but further study is required for confirmation.

In addition, Midas touch may occur during gaze shift to which head or body movements contribute significantly. For large gaze shifts of 35° or more, the angle between the head and the eyes can momentarily exceed 30°. Therefore, when the dwell time is short, placing the target in the Kuiper belt can cause Midas touch during large gaze shifts. As a countermeasure, there exists a method which increases the dwell time to distinguish between natural gaze shifts and gaze shifts that have the eye move into the Kuiper Belt like BimodalGaze [51].

8.5 Limitations

The Kuiper Belt-based menu item selection method in the VR environment is a first research prototype; so, there are limitations related to practical usage. First, the Kuiper Belt may not be suitable for spectacle wearers. The reason is that directing the gaze to the Kuiper Belt requires gazing at an area outside the eyeglasses. It is difficult for spectacle wearers to use our method with current eye-tracking technology. Similarly, eyeglass frames can interfere with the acquisition of gaze data. Thus, this method is suitable for users that do not require visual aid with the exception of contact lenses.

This is a limitation of our method; however, the technological advancements in direct retinal projection and contact lenses-styled MR hardware could eliminate this problem.

Second, as we already discussed in the section 8.1, the Kuiper Belt is not a general-purpose design principle and cannot be used for all eye-gaze interfaces (e.g. eye typing). It is difficult to place as many menu items as required for eye typing because of the low gaze accuracy and precision of the Kuiper Belt. Finally, our study design was not comprehensive to precisely investigate the characteristics of human eye-gaze movement and the Kuiper Belt. We need more variety of *iDistance* for exploring a precise form of the Kuiper Belt as well as the variety of size of menu items for a more robust and stable visual search task. We conducted our study with current design due to the time constraint for completing a study within a reasonable time. Our work is the first research to understand how we utilize the unexplored area in the eye-gaze interaction, so there are many things to consider for future research, which are our limitations and will be addressed in other study.

9 CONCLUSION

We have explored the design principle of how to place menu items in the “out-of-natural angle” region, named Kuiper Belt, of the eye-gaze interaction in a VR environment. Our idea was to utilize this “Kuiper Belt” region to solve the Midas Touch problem (false input) in the eye-gaze interface. Two studies were conducted to understand the characteristics, namely, usability and workload of the Kuiper belt-based menu item selection and visual search tasks. The results demonstrated that the region of the Kuiper Belt (Study #1) and effectiveness of Kuiper belt-based menu item selection in the VR environment (Study #2), can reduce false input (Midas touch). Physical and mental demand, and related workload indices displayed tendencies similar to the method that works within the comfort area of the eye-gaze movement. Although refinements are required for practical usage, the Kuiper Belt-based menu item selection method exhibited a significant level of performance as a first research prototype for eye tracking based menu item selection in the VR environment.

ACKNOWLEDGMENTS

This work was supported by JSPS KAKENHI Grant Number JP21H03472, The Okawa Foundation, Seiwa Foundation, The Tateisi Science and Technology Foundation, Hokkaido University Ambitious Doctoral Fellowship.

REFERENCES

- [1] Richard Abadi and Columba Scallan. 2001. Ocular oscillation on eccentric gaze. *Vision research* 41 (11 2001), 2895–907. [https://doi.org/10.1016/S0042-6989\(01\)00168-7](https://doi.org/10.1016/S0042-6989(01)00168-7)
- [2] Marc Baloup, Thomas Pietrzak, and G ry Casiez. 2019. RayCursor: A 3D Pointing Facilitation Technique Based on Raycasting. In *Proceedings of the 2019 CHI Conference on Human Factors in Computing Systems* (Glasgow, Scotland UK) (CHI '19). Association for Computing Machinery, New York, NY, USA, 1–12. <https://doi.org/10.1145/3290605.3300331>
- [3] Sebastian Boring, Marko Jurmu, and Andreas Butz. 2009. Scroll, Tilt or Move It: Using Mobile Phones to Continuously Control Pointers on Large Public Displays. In *Proceedings of the 21st Annual Conference of the Australian Computer-Human Interaction Special Interest Group: Design: Open 24/7* (Melbourne, Australia) (OZCHI '09). Association for Computing Machinery, New York, NY, USA, 161–168. <https://doi.org/10.1145/1738826.1738853>
- [4] John Brooke. 1996. SUS : A Quick and Dirty Usability Scale. *Usability Evaluation in Industry* (1996), 189–194.
- [5] Andrea Cola o, Ahmed Kirmani, Hye Soo Yang, Nan-Wei Gong, Chris Schmandt, and Vivek K. Goyal. 2013. Mime: Compact, Low Power 3D Gesture Sensing for Interaction with Head Mounted Displays. In *Proceedings of the 26th Annual ACM Symposium on User Interface Software and Technology* (St. Andrews, Scotland, United Kingdom) (UIST '13). Association for Computing Machinery, New York, NY, USA, 227–236. <https://doi.org/10.1145/2501988.2502042>
- [6] Nathan Cournia, John D. Smith, and Andrew T. Duchowski. 2003. Gaze- vs. Hand-Based Pointing in Virtual Environments. In *CHI '03 Extended Abstracts on Human Factors in Computing Systems* (Ft. Lauderdale, Florida, USA) (CHI EA '03). Association for Computing Machinery, New York, NY, USA, 772–773. <https://doi.org/10.1145/765891.765982>
- [7] Heiko Drewes and Albrecht Schmidt. 2007. Interacting with the Computer Using Gaze Gestures. In *Proceedings of the 11th IFIP TC 13 International Conference on Human-Computer Interaction - Volume Part II* (Rio de Janeiro, Brazil) (INTER-ACT'07). Springer-Verlag, Berlin, Heidelberg, 475–488.
- [8] Augusto Esteves, David Verweij, Liza Suraiya, Rasel Islam, Youryang Lee, and Ian Oakley. 2017. SmoothMoves: Smooth Pursuits Head Movements for Augmented Reality. In *Proceedings of the 30th Annual ACM Symposium on User Interface Software and Technology* (Qu bec City, QC, Canada) (UIST '17). Association for Computing Machinery, New York, NY, USA, 167–178. <https://doi.org/10.1145/3126594.3126616>
- [9] Steven Feiner, Blair MacIntyre, Marcus Haupt, and Eliot Solomon. 1993. Windows on the World: 2D Windows for 3D Augmented Reality. In *Proceedings of the 6th Annual ACM Symposium on User Interface Software and Technology* (Atlanta, Georgia, USA) (UIST '93). Association for Computing Machinery, New York, NY, USA, 145–155. <https://doi.org/10.1145/168642.168657>
- [10] Anna Maria Feit, Shane Williams, Arturo Toledo, Ann Paradiso, Harish Kulkarni, Shaun Kane, and Meredith Ringel Morris. 2017. Toward Everyday Gaze Input: Accuracy and Precision of Eye Tracking and Implications for Design. In *Proceedings of the 2017 CHI Conference on Human Factors in Computing Systems* (Denver, Colorado, USA) (CHI '17). Association for Computing Machinery, New York, NY, USA, 1118–1130. <https://doi.org/10.1145/3025453.3025599>
- [11] Tom Foulsham, Esther Walker, and Alan Kingstone. 2011. To Where, What and When of Gaze Allocation in the Lab and the Natural Environment. *Vision research* 51 (07 2011), 1920–31. <https://doi.org/10.1016/j.visres.2011.07.002>
- [12] Edward G. Freedman. 2008. Coordination of the Eyes and Head during Visual Orienting. *Experimental Brain Research* 190 (2008), 369–387.
- [13] Jeroen Goossens and John Opstal. 1997. Human Eye–Head Coordination in Two Dimensions under Different Sensorimotor Conditions. *Experimental brain research* 114 (06 1997), 542–60. <https://doi.org/10.1007/PL00005663>
- [14] Jan Gugenheimer, David Dobbstein, Christian Winkler, Gabriel Haas, and Enrico Rukzio. 2016. FaceTouch: Enabling Touch Interaction in Display Fixed UIs for Mobile Virtual Reality. In *Proceedings of the 29th Annual Symposium on User Interface Software and Technology* (Tokyo, Japan) (UIST '16). Association for Computing Machinery, New York, NY, USA, 49–60. <https://doi.org/10.1145/2984511.2984576>
- [15] Sandra G. Hart and Lowell E. Staveland. 1988. Development of NASA-TLX (Task Load Index): Results of Empirical and Theoretical Research. In *Human Mental Workload*, Peter A. Hancock and Najmedin Meshkati (Eds.). Advances in Psychology, Vol. 52. North-Holland, 139 – 183. [https://doi.org/10.1016/S0166-4115\(08\)62386-9](https://doi.org/10.1016/S0166-4115(08)62386-9)
- [16] Benjamin Hatscher, Maria Luz, Lennart E. Nacke, Norbert Elkmann, Veit M ller, and Christian Hansen. 2017. GazeTap: Towards Hands-Free Interaction in the Operating Room (ICMI '17). Association for Computing Machinery, New York, NY, USA, 243–251. <https://doi.org/10.1145/3136755.3136759>
- [17] James J. Higgins and Suleiman Tashtoush. 1994. An aligned rank transform test for interaction. *Nonlinear World* 1, 2 (1994), 201 – 211.
- [18] Juan David Hincapi -Ramos, Xiang Guo, Paymahn Moghadasian, and Pourang Irani. 2014. Consumed Endurance: A Metric to Quantify Arm Fatigue of Mid-Air Interactions. In *Proceedings of the SIGCHI Conference on Human Factors in Computing Systems* (Toronto, Ontario, Canada) (CHI '14). Association for Computing Machinery, New York, NY, USA, 1063–1072. <https://doi.org/10.1145/2556288.2557130>
- [19] Sture Holm. 1979. A Simple Sequentially Rejective Multiple Test Procedure. *Scandinavian Journal of Statistics* 6, 2 (1979), 65 – 70.
- [20] Zhiming. Hu, Sheng. Li, Congyi. Zhang, Kangrui. Yi, Guoping. Wang, and Dinesh. Manocha. 2020. DGaze: CNN-Based Gaze Prediction in Dynamic Scenes. *IEEE Transactions on Visualization and Computer Graphics* 26, 5 (2020), 1902–1911.
- [21] Yoshio Ishiguro and Jun Rekimoto. 2011. Peripheral Vision Annotation: Noninterference Information Presentation Method for Mobile Augmented Reality. In *Proceedings of the 2nd Augmented Human International Conference* (Tokyo, Japan) (AH '11). Association for Computing Machinery, New York, NY, USA, Article 8, 5 pages. <https://doi.org/10.1145/1959826.1959834>
- [22] Poika Isokoski. 2000. Text Input Methods for Eye Trackers Using Off-Screen Targets. In *Proceedings of the 2000 Symposium on Eye Tracking Research & Applications* (Palm Beach Gardens, Florida, USA) (ETRA '00). Association for Computing

- Machinery, New York, NY, USA, 15–21. <https://doi.org/10.1145/355017.355020>
- [23] Robert J. K. Jacob. 1990. What You Look at is What You Get: Eye Movement-Based Interaction Techniques. In *Proceedings of the SIGCHI Conference on Human Factors in Computing Systems* (Seattle, Washington, USA) (CHI '90). Association for Computing Machinery, New York, NY, USA, 11–18. <https://doi.org/10.1145/97243.97246>
- [24] Jorge Jimenez, Diego Gutierrez, and Pedro Latorre. 2008. Gaze-based Interaction for Virtual Environments. *Journal of Universal Computer Science* 14, 19 (nov 2008), 3085–3098.
- [25] Manu Kumar, Jeff Klingner, Rohan Puranik, Terry Winograd, and Andreas Paepcke. 2008. Improving the Accuracy of Gaze Input for Interaction. In *Proceedings of the 2008 Symposium on Eye Tracking Research & Applications* (Savannah, Georgia) (ETRA '08). Association for Computing Machinery, New York, NY, USA, 65–68. <https://doi.org/10.1145/1344471.1344488>
- [26] Manu Kumar, Andreas Paepcke, and Terry Winograd. 2007. EyePoint: Practical Pointing and Selection Using Gaze and Keyboard. In *Proceedings of the SIGCHI Conference on Human Factors in Computing Systems* (San Jose, California, USA) (CHI '07). Association for Computing Machinery, New York, NY, USA, 421–430. <https://doi.org/10.1145/1240624.1240692>
- [27] Mikko Kytö, Barrett Ens, Thammathip Piumsomboon, Gun A. Lee, and Mark Billinghurst. 2018. Pinpointing: Precise Head- and Eye-Based Target Selection for Augmented Reality. In *Proceedings of the 2018 CHI Conference on Human Factors in Computing Systems* (Montreal QC, Canada) (CHI '18). Association for Computing Machinery, New York, NY, USA, Article 81, 14 pages. <https://doi.org/10.1145/3173574.3173655>
- [28] Wallace Lages and Doug Bowman. 2019. Adjustable Adaptation for Spatial Augmented Reality Workspaces. In *Symposium on Spatial User Interaction* (New Orleans, LA, USA) (SUI '19). Association for Computing Machinery, New York, NY, USA, Article 20, 2 pages. <https://doi.org/10.1145/3357251.3358755>
- [29] Jiwon Lee, Mingyu Kim, Changyu Jeon, and Kim Jinmo. 2017. A Study on Interaction of Gaze Pointer-Based User Interface in Mobile Virtual Reality Environment. *Symmetry* 9 (09 2017), 189. <https://doi.org/10.3390/sym9090189>
- [30] Feiyu Lu, Shakiba Davari, Lee Lisle, Yuan Li, and Doug A. Bowman. 2020. Glanceable AR: Evaluating Information Access Methods for Head-Worn Augmented Reality. In *2020 IEEE Symposium on 3D User Interfaces (3DUI)*, 930–938.
- [31] Christof Lutteroth, Moiz Penkar, and Gerald Weber. 2015. Gaze vs. Mouse: A Fast and Accurate Gaze-Only Click Alternative. In *Proceedings of the 28th Annual ACM Symposium on User Interface Software & Technology* (Charlotte, NC, USA) (UIST '15). Association for Computing Machinery, New York, NY, USA, 385–394. <https://doi.org/10.1145/2807442.2807461>
- [32] Päivi Majaranta, Ulla-Kaija Ahola, and Oleg Špakov. 2009. Fast Gaze Typing with an Adjustable Dwell Time. In *Proceedings of the SIGCHI Conference on Human Factors in Computing Systems* (Boston, MA, USA) (CHI '09). Association for Computing Machinery, New York, NY, USA, 357–360. <https://doi.org/10.1145/1518701.1518758>
- [33] Päivi Majaranta and Kari-Jouko Räihä. 2002. Twenty Years of Eye Typing: Systems and Design Issues. In *Proceedings of the 2002 Symposium on Eye Tracking Research & Applications* (New Orleans, Louisiana) (ETRA '02). Association for Computing Machinery, New York, NY, USA, 15–22. <https://doi.org/10.1145/507072.507076>
- [34] Päivi Majaranta and Kari-Jouko Räihä. 2007. *Text Entry by Gaze: Utilizing Eye-Tracking*, 175–187.
- [35] Diako. Mardanbegi, Benedikt. Mayer, Ken. Pfeuffer, Shahram. Jalaliniya, Hans. Gellersen, and Alexander. Perzl. 2019. EyeSeeThrough: Unifying Tool Selection and Application in Virtual Environments. In *2019 IEEE Conference on Virtual Reality and 3D User Interfaces (VR)*, 474–483.
- [36] Pranav Mistry and Pattie Maes. 2009. SixthSense: A Wearable Gestural Interface. In *ACM SIGGRAPH ASIA 2009 Sketches* (Yokohama, Japan) (SIGGRAPH ASIA '09). Association for Computing Machinery, New York, NY, USA, Article 11, 1 pages. <https://doi.org/10.1145/1667146.1667160>
- [37] Martez E. Mott, Shane Williams, Jacob O. Wobbrock, and Meredith Ringel Morris. 2017. Improving Dwell-Based Gaze Typing with Dynamic, Cascading Dwell Times. In *Proceedings of the 2017 CHI Conference on Human Factors in Computing Systems* (Denver, Colorado, USA) (CHI '17). Association for Computing Machinery, New York, NY, USA, 2558–2570. <https://doi.org/10.1145/3025453.3025517>
- [38] Florian Müller, Joshua McManus, Sebastian Günther, Martin Schmitz, Max Mühlhäuser, and Markus Funk. 2019. Mind the Tap: Assessing Foot-Taps for Interacting with Head-Mounted Displays. In *Proceedings of the 2019 CHI Conference on Human Factors in Computing Systems* (Glasgow, Scotland UK) (CHI '19). Association for Computing Machinery, New York, NY, USA, Article 477, 13 pages. <https://doi.org/10.1145/3290605.3300707>
- [39] Abdul Moiz Penkar, Christof Lutteroth, and Gerald Weber. 2012. Designing for the Eye: Design Parameters for Dwell in Gaze Interaction. In *Proceedings of the 24th Australian Computer-Human Interaction Conference* (Melbourne, Australia) (OzCHI '12). Association for Computing Machinery, New York, NY, USA, 479–488. <https://doi.org/10.1145/2414536.2414609>
- [40] Ken Pfeuffer, Yasmeen Abdrabou, Augusto Esteves, Radiah Rivu, Yomna Abdelrahman, Stefanie Meitner, Amr Saadi, and Florian Alt. 2021. ARtention: A design space for gaze-adaptive user interfaces in augmented reality. *Computers & Graphics* 95 (2021), 1–12. <https://doi.org/10.1016/j.cag.2021.01.001>
- [41] Ken Pfeuffer, Benedikt Mayer, Diako Mardanbegi, and Hans Gellersen. 2017. Gaze + Pinch Interaction in Virtual Reality. In *Proceedings of the 5th Symposium on Spatial User Interaction* (Brighton, United Kingdom) (SUI '17). Association for Computing Machinery, New York, NY, USA, 99–108. <https://doi.org/10.1145/3131277.3132180>
- [42] Jimin Pi and Bertram E. Shi. 2017. Probabilistic Adjustment of Dwell Time for Eye Typing. In *2017 10th International Conference on Human System Interactions (HSI)*, 251–257.
- [43] Argenis Ramirez Ramirez Gomez, Christopher Clarke, Ludwig Sidenmark, and Hans Gellersen. 2021. Gaze+Hold: Eyes-Only Direct Manipulation with Continuous Gaze Modulated by Closure of One Eye. In *ACM Symposium on Eye Tracking Research and Applications* (Virtual Event, Germany) (ETRA '21 Full Papers). Association for Computing Machinery, New York, NY, USA, Article 10, 12 pages. <https://doi.org/10.1145/3448017.3457381>
- [44] Houssein Saidi, Emmanuel Dubois, and Marcos Serrano. 2021. *HoloBar: Rapid Command Execution for Head-Worn AR Exploiting Around the Field-of-View Interaction*. Association for Computing Machinery, New York, NY, USA. <https://doi.org/10.1145/3411764.3445255>
- [45] K. C. Salter and R. F. Fawcett. 1993. The art test of interaction: a robust and powerful rank test of interaction in factorial models. *Communications in Statistics - Simulation and Computation* 22, 1 (1993), 137–153. <https://doi.org/10.1080/03610919308813085>
- [46] Simon Schenk, Philipp Tiefenbacher, Gerhard Rigoll, and Michael Dorr. 2016. SPOCK: A Smooth Pursuit Oculomotor Control Kit. In *Proceedings of the 2016 CHI Conference Extended Abstracts on Human Factors in Computing Systems* (San Jose, California, USA) (CHI EA '16). Association for Computing Machinery, New York, NY, USA, 2681–2687. <https://doi.org/10.1145/2851581.2892291>
- [47] Linda E. Sibert and Robert J. K. Jacob. 2000. Evaluation of Eye Gaze Interaction. In *Proceedings of the SIGCHI Conference on Human Factors in Computing Systems* (The Hague, The Netherlands) (CHI '00). Association for Computing Machinery, New York, NY, USA, 281–288. <https://doi.org/10.1145/332040.332445>
- [48] Ludwig Sidenmark, Christopher Clarke, Xuesong Zhang, Jenny Phu, and Hans Gellersen. 2020. Outline Pursuits: Gaze-Assisted Selection of Occluded Objects in Virtual Reality. In *Proceedings of the 2020 CHI Conference on Human Factors in Computing Systems* (Honolulu, HI, USA) (CHI '20). Association for Computing Machinery, New York, NY, USA, 1–13. <https://doi.org/10.1145/3313831.3376438>
- [49] Ludwig Sidenmark and Hans Gellersen. 2019. Eye & Head: Synergetic Eye and Head Movement for Gaze Pointing and Selection. In *Proceedings of the 32nd Annual ACM Symposium on User Interface Software and Technology* (New Orleans, LA, USA) (UIST '19). Association for Computing Machinery, New York, NY, USA, 1161–1174. <https://doi.org/10.1145/3332165.3347921>
- [50] Ludwig Sidenmark and Hans Gellersen. 2019. Eye, Head and Torso Coordination During Gaze Shifts in Virtual Reality. *ACM Trans. Comput.-Hum. Interact.* 27, 1, Article 4 (Dec. 2019), 40 pages. <https://doi.org/10.1145/3361218>
- [51] Ludwig Sidenmark, Diako Mardanbegi, Argenis Ramirez Gomez, Christopher Clarke, and Hans Gellersen. 2020. BimodalGaze: Seamlessly Refined Pointing with Gaze and Filtered Gestural Head Movement. In *Symposium on Eye Tracking Research and Applications* (Stuttgart, Germany) (ETRA '20). Association for Computing Machinery, New York, NY, USA, Article 8, 9 pages. <https://doi.org/10.1145/3379155.3391312>
- [52] Ludwig Sidenmark, Dominic Potts, Bill Bapich, and Hans Gellersen. 2021. *RadiEye: Hands-Free Radial Interfaces for 3D Interaction Using Gaze-Activated Head-Crossing*. Association for Computing Machinery, New York, NY, USA. <https://doi.org/10.1145/3411764.3445697>
- [53] John Stahl. 2001. Eye-Head Coordination and the Variation of Eye-Movement Accuracy with Orbital Eccentricity. *Experimental brain research. Experimentelle Hirnforschung. Expérimentation cérébrale* 136 (02 2001), 200–10. <https://doi.org/10.1007/s002210000593>
- [54] John S. Stahl. 1999. Amplitude of Human Head Movements Associated with Horizontal Saccades. *Experimental Brain Research* 126 (1999), 41–54.
- [55] Veikko Surakka, Marko Illi, and Poika Isokoski. 2004. Gazing and Frowning as a New Human-Computer Interaction Technique. *ACM Trans. Appl. Percept.* 1, 1 (July 2004), 40–56. <https://doi.org/10.1145/1008722.1008726>
- [56] Vildan Tanriverdi and Robert J. K. Jacob. 2000. Interacting with Eye Movements in Virtual Environments. In *Proceedings of the SIGCHI Conference on Human Factors in Computing Systems* (The Hague, The Netherlands) (CHI '00). Association for Computing Machinery, New York, NY, USA, 265–272. <https://doi.org/10.1145/332040.332443>
- [57] Marcus Tönnis and Gudrun Klinker. 2014. Boundary Conditions for Information Visualization with Respect to the User's Gaze. In *Proceedings of the 5th Augmented Human International Conference* (Kobe, Japan) (AH '14). Association for Computing Machinery, New York, NY, USA, Article 44, 8 pages. <https://doi.org/10.1145/2582051.2582095>
- [58] Mélodie Vidal, Andreas Bulling, and Hans Gellersen. 2013. Pursuits: Spontaneous Interaction with Displays Based on Smooth Pursuit Eye Movement and Moving Targets. In *Proceedings of the 2013 ACM International Joint Conference on Pervasive*

- and *Ubiquitous Computing* (Zurich, Switzerland) (*UbiComp '13*). Association for Computing Machinery, New York, NY, USA, 439–448. <https://doi.org/10.1145/2493432.2493477>
- [59] Oleg Špakov and Darius Miniotas. 2004. On-Line Adjustment of Dwell Time for Target Selection by Gaze. In *Proceedings of the Third Nordic Conference on Human-Computer Interaction* (Tampere, Finland) (*NordiCHI '04*). Association for Computing Machinery, New York, NY, USA, 203–206. <https://doi.org/10.1145/1028014.1028045>
- [60] Colin Ware and Harutune H. Mikaelian. 1986. An Evaluation of an Eye Tracker as a Device for Computer Input. *SIGCHI Bull.* 18, 4 (May 1986), 183–188. <https://doi.org/10.1145/1165387.275627>
- [61] Jacob O. Wobbrock, Leah Findlater, Darren Gergle, and James J. Higgins. 2011. The Aligned Rank Transform for Nonparametric Factorial Analyses Using Only Anova Procedures. In *Proceedings of the SIGCHI Conference on Human Factors in Computing Systems* (Vancouver, BC, Canada) (*CHI '11*). ACM, New York, NY, USA, 143–146. <https://doi.org/10.1145/1978942.1978963>
- [62] Wenge Xu, Hai-Ning Liang, Yuxuan Zhao, Difeng Yu, and Diego Monteiro. 2019. DMove: Directional Motion-Based Interaction for Augmented Reality Head-Mounted Displays. In *Proceedings of the 2019 CHI Conference on Human Factors in Computing Systems* (Glasgow, Scotland Uk) (*CHI '19*). Association for Computing Machinery, New York, NY, USA, Article 444, 14 pages. <https://doi.org/10.1145/3290605.3300674>
- [63] Lijing Yao and C. K. Peck. 1997. Saccadic eye movements to visual and auditory targets. *Experimental brain research* 115 (06 1997), 25–34. <https://doi.org/10.1007/PL00005682>
- [64] Difeng Yu, Hai-Ning Liang, Xueshi Lu, Kaixuan Fan, and Barrett Ens. 2019. Modeling Endpoint Distribution of Pointing Selection Tasks in Virtual Reality Environments. *ACM Trans. Graph.* 38, 6, Article 218 (Nov. 2019), 13 pages. <https://doi.org/10.1145/3355089.3356544>
- [65] Shumin Zhai, Carlos Morimoto, and Steven Ihde. 1999. Manual and Gaze Input Cascaded (MAGIC) Pointing. In *Proceedings of the SIGCHI Conference on Human Factors in Computing Systems* (Pittsburgh, Pennsylvania, USA) (*CHI '99*). Association for Computing Machinery, New York, NY, USA, 246–253. <https://doi.org/10.1145/302979.303053>
- [66] Xinyong Zhang, Pianpian Xu, Qing Zhang, and Hongbin Zha. 2011. Speed-Accuracy Trade-off in Dwell-Based Eye Pointing Tasks at Different Cognitive Levels. In *Proceedings of the 1st International Workshop on Pervasive Eye Tracking & Mobile Eye-Based Interaction* (Beijing, China) (*PETMEI '11*). Association for Computing Machinery, New York, NY, USA, 37–42. <https://doi.org/10.1145/2029956.2029967>
- [67] Xiaoyu (Amy) Zhao, Elias D. Guestrin, Dimitry Sayenko, Tyler Simpson, Michel Gauthier, and Milos R. Popovic. 2012. Typing with Eye-Gaze and Tooth-Clicks. In *Proceedings of the Symposium on Eye Tracking Research and Applications* (Santa Barbara, California) (*ETRA '12*). Association for Computing Machinery, New York, NY, USA, 341–344. <https://doi.org/10.1145/2168556.2168632>